

# A Uniformly Convergent Approximation for Ideal Complex Half-Band Filters

Gagan Mirchandani\*

School of Engineering, The University of Vermont, Burlington, VT 05405  
mirchand@cems.uvm.edu, (802)656-4587, (802)656-3358 (Fax)

Mohamed Elfataoui

melfatao@cems.uvm.edu, (802)656-4034, (802)656-3358 (Fax)  
School of Engineering, The University of Vermont, Burlington, VT 05405

July 14, 2006

## Abstract

In contrast to the well known and classic frequency domain method for generating a discrete-time analytic signal, we show that the same signal can also be generated using a real-time complex half-band FIR filter. More significantly, we show that the spectrum of the  $N$  length filter ( $N$  a multiple of 4) converges uniformly to the ideal complex half-band spectrum as  $N \rightarrow \infty$ , except away from the discontinuities at 0 and  $\pi$ , where it converges pointwise. The filter design, in contrast to some other methods, is easily scalable and stable. Furthermore, we derive the closed form expression of the filter frequency response. For evaluating filter performance, we focus on the spacial shiftability property of the filter and compare it with that of other filter designs. Using a total variation measure for determining function variation, we see that shiftability is excellent for an impulse input and better on average, with other inputs.

EDICS names: DSP-FILT, DSP-TFSR

---

\*Supported in part by DEPSCoR Grant No.F49620-00-1-0280

## I. INTRODUCTION

Of the many ways for generating discrete-time analytic (DTA) signals, one of the more popular techniques is to use the MATLAB function *hilbert*. This is a non real-time frequency domain approach [8] where the spectrum of the signal is operated on in a particular way. We show that the same DTA signal can be generated with a real-time complex half-band FIR filter - derived using the frequency domain approach. The main contribution of this paper is the following: the amplitude spectrum of the  $N$ -point half-band FIR filter approximation converges uniformly to that of the ideal complex half-band filter as  $N \rightarrow \infty$  ( $N$  a multiple of 4). In contrast to the expressions for impulse response coefficients for various standard ideal filters [9], p.528) we formulate a closed form expression in frequency of the  $N$ -point filter. This can often provide an analytic foothold into filter design. We also measure the deviation of the approximation from the ideal zero spectrum in  $(-\pi, 0)$  and compare with that by other methods. Since the frequency domain method lends itself to an extension, we also measure deviation from the ideal using that extension.

The ideal complex half-band filter and the ideal DTA signal have frequency responses that are zero for  $\omega \in (-\pi, 0)$ . The ideal filter has in addition, constant amplitude for  $\omega \in (0, \pi)$ . (The definition of half-band and complex half-band is recalled in Section III).  $N$ -point FIR approximations to the ideal complex half-band filter will henceforth be referred to as complex filters. They will be called half-band complex filters when the corresponding lowpass filter has the half-band property. In such a case we will loosely refer to the complex filter as also being half-band even though it is the lowpass that has the half-band property. Approximations to the ideal DTA signal will be called DTA signals or just analytic signals. We provide a brief background of the existing techniques for DTA signal generation in Section II. The new method and the closed form expression of the frequency response is described in Section III. Convergence established in Section IV. Experimental results and conclusions are given in Sections V and VI respectively.

## II. BACKGROUND

The first method for generating DTA signals is in the frequency domain. This classic method is described in [8], [5] and implemented by the MATLAB 7 algorithm *hilbert*. Discrete Fourier transform (DFT) coefficients of the given real signal are modified in a simple way: Discrete negative frequency terms, that is, those lying in  $-\pi < \omega < 0$  are set to zero. Discrete positive frequency terms lying in  $0 \leq \omega \leq \pi$  are multiplied by 2, except those at the end-points  $0, \pi$ , which are multiplied by 1. The inverse DFT (IDFT) of the modified signal yields the analytic signal. An extension to this technique is described in [1], [2], [3] and referred to as *ehilbert*.

The second method for DTA signal generation requires generation of lowpass filters or Hilbert transformers. In the former case, the lowpass filter spectrum is shifted to the right by  $\pi/2$  to generate complex filters. In the two methods described here, these filters are not half-band. In the first of these methods, the lowpass filter is an “optimal” Daubechies scaling filter [4]. The second lowpass method uses an equiripple approximation ([9] p.895). Here, the FIR lowpass filter is an equiripple design. The other filter design procedure which results in complex half-band filters, entails Hilbert transformers. In the first of these methods the ideal Hilbert transformer is approximated using the Fourier series representation and a Kaiser window ([10] p.793). The second method uses an equiripple approximation ([9] p.895).

### III. FILTER DESIGN AND CLOSED FORM EXPRESSION

We first recall the definition of half-band. The ideal frequency response for our purposes here is

$$G(e^{j\omega}) = \begin{cases} 2, & 0 < \omega < \pi \\ 0, & -\pi < \omega < 0. \end{cases} \quad (1)$$

As described in (ibid., 895) Equation (1) describes a *complex half-band filter* since shifting its frequency response left by  $\pi/2$  generates a (lowpass) real filter  $H(e^{j\omega})$  satisfying the property of *half-band* (ibid., 783). That is

$$H(e^{j\omega}) = \frac{1}{2}G(e^{j(\omega+\pi/2)}) \begin{cases} 1, & 0 < |\omega| < \pi/2 \\ 0, & \pi/2 < |\omega| < \pi \end{cases} \quad (2)$$

where, for the zero phase half-band case we have

$$H(z) = \alpha + z^{-1}E_1(z^2) \quad (3)$$

and

$$h[2n] = \begin{cases} \alpha, & n = 0 \\ 0, & \text{otherwise} \end{cases} \quad (4)$$

and typically  $\alpha = 1$ . Equation (3) then generates the well known half-band property  $H(z) + H(-z) = 1$ . FIR approximations to the ideal filters of equations (1) and (2) satisfying the half-band property, will likewise be referred to as complex half-band or half-band respectively.

The filter design procedure proceeds as follows: We start with an impulse function of length  $N$ , shifted by  $N/2$  when the filter length is even. (Or  $((N-1)/2)$  when the length odd). The choice of the shift assures generalized linear phase. This delayed impulse is operated on by the function *hilbert* [8] to generate the DTA signal of an impulse. These signal coefficients constitute the impulse response of the approximation to the ideal complex half-band filter.

The closed form expression of the complex filter frequency response  $Z(e^{j\omega})$  is obtained after deriving the closed form expression of the impulse response  $z(n)$  of the filter. We first consider output  $z(n)$  for the general case where  $x(n)$  is an arbitrary discrete-time real signal.

#### A. Input-output relationship when $N$ is even

Let  $x(n)$  be a discrete-time real signal of length  $N$ , where  $N$  is even. Subjecting  $x(n)$  to the frequency domain method [8], we get output  $z(n)$ . The expression for  $z(n)$  of the DTA signal corresponding to  $x(n)$ , [[2], Eqs. (1), (2)], [1], [3] is given by the following equation:

$$z(n) = \begin{cases} x(n) + j\left(\frac{2}{N}\right) \sum_{p=0}^{N/2-1} x(2p+1) \cot(\pi(n-(2p+1))/N), & \text{for } n \text{ even} \\ x(n) + j\left(\frac{2}{N}\right) \sum_{p=0}^{N/2-1} x(2p) \cot(\pi(n-2p)/N), & \text{for } n \text{ odd.} \end{cases} \quad (5)$$

*B. Impulse response when  $N$  is even,  $N$  multiple of 4*

Let  $x(n)$  be the discrete-time impulse of length  $N$ , shifted by  $N/2$ , that is  $x(n) = 1, n = N/2$  and 0 otherwise. Using equation (5) with  $x(n)$  as above, we obtain the expression for the impulse response  $z(n)$  of the DTA signal. This is the same signal that would be obtained were we to apply algorithm [8] to  $x(n)$  above. Hence

$$z(n) = \begin{cases} 0, & n \text{ even, } n \neq N/2 \\ 1, & n = N/2 \\ j(\frac{2}{N}) \cot(\frac{\pi}{N}n - \frac{\pi}{2}), & n \text{ odd.} \end{cases} \quad (6)$$

We note the efficiency of the representation here. The only non-zero even indexed element of  $x(n)$  is at  $n = N/2$  and is equal to 1. The other cases for  $N$  even and  $N/2$  odd, as also  $N$  odd, are omitted for brevity. We observe here that the impulse response coefficients for  $z(n)$ , given by equation (6) has the half-band property in that all alternating coefficients except one are zero. However, it is easily seen that equation(4) defining the half-band property is satisfied exactly when the filter coefficients are centered about  $N/2$ .

The frequency response  $Z(e^{j\omega})$  can now be determined. The closed form expression for  $N$  a multiple of 4 is derived in Appendix A and shown below. The other cases of ( $N$  even and  $N/2$  odd) and  $N$  odd, are also included here, although the proof is omitted for brevity:

$$Z(e^{j\omega}) = \begin{cases} e^{-j\omega N/2} \{1 + \frac{4}{N} \sum_{n=0}^{\frac{N}{4}-1} \tan(\frac{\pi}{N}(2n+1)) \sin(\omega(\frac{N}{2} - (2n+1)))\}, & \text{for } N \text{ even, } N \text{ multiple of 4} \\ e^{-j\omega N/2} \{1 + \frac{4}{N} \sum_{n=1}^{\frac{1}{2}(\frac{N}{2}-1)} \tan(\frac{\pi}{N}2n) \sin(\omega(\frac{N}{2} - 2n))\}, & \text{for } N \text{ even, } N/2 \text{ odd} \\ e^{-j\omega \frac{N-1}{2}} \{1 + \frac{2}{N} \sum_{n=1}^{\frac{N-1}{2}} \frac{\cos(\frac{\pi n}{N}) - (-1)^n}{\sin(\frac{\pi n}{N})} \sin(n\omega)\}, & \text{for } N \text{ odd.} \end{cases} \quad (7)$$

#### IV. CONVERGENCE

We now show that  $|Z(e^{j\omega})|$  converges uniformly to the function in equation (1). The proof is available for  $N$  even,  $N$  a multiple of 4. Other cases, (i)  $N$  is even and  $N/2$  odd and (ii)  $N$  is odd, are presently under investigation.

**Theorem 1:** For  $N$  a multiple of 4, the function

$$|Z(e^{j\omega})| = |1 + \frac{4}{N} \sum_{n=0}^{\frac{N}{4}-1} \tan(\frac{\pi}{N}(2n+1)) \sin(\omega(\frac{N}{2} - (2n+1)))|$$

converges uniformly away from the two discontinuities to  $G(e^{j\omega})$  given by equation (1). At discontinuities  $\omega = 0, \pi$ ,  $|Z(e^{j\omega})|$  converges pointwise to 1.

**Proof:** The proof is given in Appendix B.

## V. EXPERIMENTAL RESULTS

As a measure of filter performance, we determine the degree of attenuation in the region  $(-\pi, 0)$ , or equivalently, the aliasing generated when the filter output is downsampled. This can be measured in many ways: through determining stopband energies, peak ripple, mean-square error and so on. We focus instead on a measure of the use of the analytic signal when applied to orthogonal wavelet filter banks. That is, we measure the aliasing generated when the DTA signal is subsampled. Such applications occur in the design of complex wavelets [12]. Aliasing is measured using shiftability [13] with respect to all input signals (ibid., Proposition (2)). That is, input signals are applied to a critically sampled wavelet filter bank and coefficient energy at each subband level is measured as the input signal is cyclically translated. Constant subband-energy implies shiftability. For our purposes here, the DTA signals generated from various inputs to the complex filters are applied to the filter bank and shiftability measured. In this way we compare shiftability of all the filters described, with that by the new method.

Aliasing generated will of course depend on the spectral characteristics of the input signal. As a simple solution to the difficult signal selection problem, we choose signals previously used in the literature for measuring shiftability. Accordingly, we employ an impulse function [4], step function [6], and a fractal signal [13].

In our experiments we use a critically sampled, orthogonal wavelet filter bank using the *db8* wavelet family at  $M$ -levels. This particular filter bank is chosen since it has been shown ([4], Sec.3.3, Proposition 1) that using the Strang-Nguyen model [[14], p.172] for the Daubechies scaling filter at  $M$  level, and using a Daubechies complex filter of length  $N$  satisfying the conditions of Proposition 1, full shiftability is obtained. Accordingly we compare performance of all our complex filters using this model: A critically sampled, orthogonal wavelet filter bank using the *db8* wavelet family and complex filters of size  $N = 28$  with  $M = 3$ . When the filter size needs to be odd, we use  $N = 27$ . The MATLAB 7 expression *wfilters('db8')* generates the filter bank. Therefore Proposition 1 that entails conditions on  $N$ ,  $M$  and filter bank wavelet length is satisfied.

Complex filters were generated by the following five methods: The first one using a lowpass Daubechies (LP\_daub) scaling filter (from *db14*) of length 28 shifted by  $\pi/2$  [4]. Another from a lowpass filter [11] (LP\_equiripple) of length 27 and transition band width of  $0.16\pi$  using the function *firpm* in MATLAB 7. Two Hilbert transformers of length  $N = 27$  were generated and then complex half-band filters formed, using the basic scheme referred to earlier for generation of analytic signals. The first (HT\_equiripple) ([10], pp. 792-794) was designed using the function *firpm* with the option *Hilbert* and the passband frequency range  $[0.1\pi, 0.9\pi]$ . The second (HT\_windowed) (ibid., 793) was a Fourier series approximation with a Kaiser window, using  $\beta = 3.227$ . This was derived using the minimum attenuation between 21 and 50 dB. Finally, for the new method, a length 27 complex filter was generated. We note that an impulse of length 28 was used. Since, by equation (6), the first element of the DTA signal is zero, we consider the length as 27. Figure (1) shows the normalized magnitude frequency response of the five filters.

All five filters were used to generate DTA signals corresponding to input signals - impulse, step and fractal. Subband-energy was measured at the 3 levels of a critically sampled orthogonal wavelet filter bank using the *db8* wavelet family, over 16 circular shifts of the input signals.

To obtain a quantitative measure of performance, we determine the variation of subband-energy using the concept of total variation [7]. The latter is defined as  $TV = \sum_{k=1}^{16} |x_k - x_{k-1}|$ , where  $x_i$  represents subband-energy. We use the ratio of TV\_new method and TV\_other method for comparison. Hence small numbers indicate a better performance. Results are shown in Table 1 for the impulse function, Table 2 for the step function and Table 3 for the fractal signal. We observe better performance with the new method in 35 of the 48 simulations.

Improved shiftability, that is a further reductions in aliasing, can be obtained by applying *ehilbert* [2] instead of *hilbert* to the delayed input impulse. We choose to zero the negative spectrum at an additional negative frequency  $\omega = -2.0415$ , which is determined empirically. The ratio TV\_ehilbert and TV\_hilbert is used for comparison here. Results are shown in Table 4 for an input impulse function. It is observed that in using *ehilbert* with the new method, we further reduce aliasing at all levels except that at Level-2 highpass, where the results are close.

The new method is efficient since for the case  $N$  even, about half the filter coefficients are equal to zero, as seen in equation (6). The other methods where the same efficiency occurs, is in HT\_windowed and HT\_equiripple. We observed in the simulations that in the latter method the “zero” coefficients, while small, are typically never zero nor infinitesimal. This has been pointed out before ([9] p.896). We have also observed that the HT\_equiripple design using the MATLAB 7 function *firpm* is not stable for large  $N$ , as also concluded in [11]. Both these problems are due to the recursive nature of the algorithm which causes roundoff errors. In the new method, “zero” filter coefficient values are indeed exactly zero and the method is stable for all  $N$ .

## VI. CONCLUSION

A simple method for generating FIR complex filters, that approximate the ideal complex half-band filter, has been proposed. We have shown that for  $N$  even and a multiple of 4, the  $N$ -point FIR filter frequency response converges uniformly to the frequency response of an ideal complex half-band filter as  $N \rightarrow \infty$ , except away from the discontinuities at 0 and  $\pi$  where it converges pointwise. A closed form expression for the filter frequency response is derived. The filter has half-band properties and is stable for large  $N$ . The shiftability property is excellent for an impulse input and better than average for other inputs. Further improvement in shiftability can be obtained using the extension *ehilbert*.

## APPENDIX A EXPRESSION FOR $Z(e^{j\omega})$

We calculate the DTFT  $Z(e^{j\omega})$  of  $z(n)$ ,  $N$  a multiple of 4. Using equation (6) we have

$$\begin{aligned} Z(e^{j\omega}) &= \sum_{n=0}^{N-1} z(n)e^{-j\omega n} = \sum_{n=0}^{\frac{N}{2}-1} z(2n+1)e^{-j\omega(2n+1)} + e^{-j\omega N/2} \\ &= \sum_{n=0}^{\frac{N}{4}-1} z(2n+1)e^{-j\omega(2n+1)} + \sum_{n=N/4}^{\frac{N}{2}-1} z(2n+1)e^{-j\omega(2n+1)} + e^{-j\omega N/2}. \end{aligned}$$

Therefore

$$\begin{aligned}
Z(e^{j\omega}) &= \{(z(1)e^{-j\omega} + z(N-1)e^{-j(N-1)\omega}) + (z(3)e^{-j3\omega} + z(N-3)e^{-j(N-3)\omega}) \\
&\quad + \dots + (z(\frac{N}{2}-1)e^{-j(\frac{N}{2}-1)\omega} + z(\frac{N}{2}+1)e^{-j(\frac{N}{2}+1)\omega})\} + e^{-j\omega N/2} \\
&= \{(z(1)e^{-j\omega} + z(N-1)e^{-j(N-1)\omega}) + (z(3)e^{-j3\omega} + z(N-3)e^{-j(N-3)\omega}) \\
&\quad + \dots + (z(\frac{N}{2}-1)e^{-j(\frac{N}{2}-1)\omega} + z(\frac{N}{2}+1)e^{-j(N-(\frac{N}{2}-1))\omega})\} + e^{-j\omega N/2}.
\end{aligned} \tag{8}$$

We now show that for  $1 \leq 2n+1 \leq N/2$ , with  $0 \leq n \leq N/2-1$ ,  $z(N-(2n+1)) = -z(2n+1)$ .

Since  $(N-(2n+1))$  is odd, equation (6) implies

$$\begin{aligned}
z(N-(2n+1)) &= j(2/N)\cot(\frac{\pi}{N}(N-(2n+1)) - \frac{\pi}{2}) = j(2/N)\cot(\pi - \frac{\pi}{N}(2n+1) - \frac{\pi}{2}) \\
&= j(2/N)\cot(\pi/2 - \frac{\pi}{N}(2n+1)) = -j(2/N)\cot(\frac{\pi}{N}(2n+1) - \pi/2) = -z(2n+1).
\end{aligned}$$

Therefore equation (8) becomes

$$\begin{aligned}
Z(e^{j\omega}) &= \{(z(1)e^{-j\omega} - z(1)e^{-j(N-1)\omega}) + (z(3)e^{-j3\omega} - z(3)e^{-j(N-3)\omega}) + \dots + \\
&\quad (z(\frac{N}{2}-1)e^{-j(\frac{N}{2}-1)\omega} - z(\frac{N}{2}-1)e^{-j(N-(\frac{N}{2}-1))\omega})\} + e^{-j\omega N/2} \\
&= \{z(1)(e^{-j\omega} - e^{-j(N-1)\omega}) + z(3)(e^{-j3\omega} - e^{-j(N-3)\omega}) + \dots + \\
&\quad z(\frac{N}{2}-1)(e^{-j(\frac{N}{2}-1)\omega} - e^{-j(N-(\frac{N}{2}-1))\omega})\} + e^{-j\omega N/2} \\
&= e^{-j\omega N/2}\{1 + z(1)(e^{j\omega(\frac{N}{2}-1)} - e^{-j\omega(\frac{N}{2}-1)}) + z(3)(e^{j\omega(\frac{N}{2}-3)} \\
&\quad - e^{-j\omega(\frac{N}{2}-3)}) + \dots + z(\frac{N}{2}-1)(e^{j\omega} - e^{-j\omega})\} \\
&= e^{-j\omega N/2}\{1 + 2jz(1)\sin(\omega(\frac{N}{2}-1)) + 2jz(3)\sin(\omega(\frac{N}{2}-3)) \\
&\quad + \dots + 2jz(\frac{N}{2}-1)\sin(\omega)\} \\
&= e^{-j\omega N/2}\{1 + 2j \sum_{n=0}^{\frac{N}{4}-1} z(2n+1)\sin(\omega(\frac{N}{2} - (2n+1)))\}.
\end{aligned}$$

We now substitute for  $z(n+1)$ , its value given by equation (6). Hence

$$\begin{aligned}
Z(e^{j\omega}) &= e^{-j\omega N/2}\{1 + 2j \sum_{n=0}^{\frac{N}{4}-1} j(2/N)\cot(\frac{\pi}{N}(2n+1) - \frac{\pi}{2})\sin(\omega(\frac{N}{2} - (2n+1)))\} \\
&= e^{-j\omega N/2}\{1 - \frac{4}{N} \sum_{n=0}^{\frac{N}{4}-1} \cot(\frac{\pi}{N}(2n+1) - \frac{\pi}{2})\sin(\omega(\frac{N}{2} - (2n+1)))\}
\end{aligned}$$

$$= e^{-j\omega N/2} \left\{ 1 + \frac{4}{N} \sum_{n=0}^{\frac{N}{4}-1} \tan\left(\frac{\pi}{N}(2n+1)\right) \sin\left(\omega\left(\frac{N}{2} - (2n+1)\right)\right) \right\}.$$

Including results (proof omitted here) for the two other values of  $N$ , we have

$$Z(e^{j\omega}) = \begin{cases} e^{-j\omega N/2} \left\{ 1 + \frac{4}{N} \sum_{n=0}^{\frac{N}{4}-1} \tan\left(\frac{\pi}{N}(2n+1)\right) \sin\left(\omega\left(\frac{N}{2} - (2n+1)\right)\right) \right\}, & N \text{ multiple of 4} \\ e^{-j\omega N/2} \left\{ 1 + \frac{4}{N} \sum_{n=1}^{\frac{1}{2}(\frac{N}{2}-1)} \tan\left(\frac{\pi}{N}2n\right) \sin\left(\omega\left(\frac{N}{2} - 2n\right)\right) \right\}, & N \text{ even, } N/2 \text{ odd} \\ e^{-j\omega \frac{N-1}{2}} \left\{ 1 + \frac{2}{N} \sum_{n=1}^{\frac{N-1}{2}} \frac{\cos\left(\frac{\pi n}{N}\right) - (-1)^n}{\sin\left(\frac{\pi n}{N}\right)} \sin(n\omega) \right\}, & N \text{ odd.} \end{cases} \quad (9)$$

## APPENDIX B PROOF OF THEOREM 1

First we prove that for the region  $\omega \in \{(0, \pi), (-\pi, 0)\}$

$$|Z(e^{j\omega})| = \left| 1 + \frac{4}{N} \sum_{n=0}^{\frac{N}{4}-1} \tan\left(\frac{\pi}{N}(2n+1)\right) \sin\left(\omega\left(\frac{N}{2} - (2n+1)\right)\right) \right|$$

converges uniformly to  $G(e^{j\omega})$  given by equation (1), when  $N \rightarrow +\infty$  and  $N$  a multiple of 4. Convergence at the discontinuities is established after that. By using a change of variable  $k = \frac{N}{4} - 1 - n$ , we get

$$|Z(e^{j\omega})| = \left| 1 + \frac{4}{N} \sum_{n=0}^{\frac{N}{4}-1} \cot\left(\frac{\pi}{N}(2n+1)\right) \sin(\omega(2n+1)) \right| = |1 + f(\omega)|$$

where

$$f(\omega) = \frac{4}{N} \sum_{n=0}^{\frac{N}{4}-1} \cot\left(\frac{\pi}{N}(2n+1)\right) \sin(\omega(2n+1)).$$

Then it is sufficient to prove that  $f(\omega)$  converge to 1 on  $(0, \pi)$  and to 0 on  $(-\pi, 0)$  everywhere and uniformly when  $N \rightarrow \infty$ . We have

$$\begin{aligned} f(\omega) &= \frac{4}{N} \sum_{n=0}^{\frac{N}{4}-1} \cot\left(\frac{\pi}{N}(2n+1)\right) \sin(\omega(2n+1)) \\ &= \frac{4}{N} \sum_{n=0}^{\frac{N}{4}-1} \left\{ \left\{ \cot\left(\frac{\pi}{N}(2n+1)\right) - \frac{N}{\pi(2n+1)} \right\} \sin(\omega(2n+1)) \right\} + \frac{4}{N} \sum_{n=0}^{\frac{N}{4}-1} \frac{N}{\pi(2n+1)} \sin(\omega(2n+1)) \\ &= \frac{4}{N} \sum_{n=0}^{\frac{N}{4}-1} \left\{ \left\{ \cot\left(\frac{\pi}{N}(2n+1)\right) - \frac{N}{\pi(2n+1)} \right\} \sin(\omega(2n+1)) \right\} + \frac{4}{\pi} \sum_{n=0}^{\frac{N}{4}-1} \frac{\sin(\omega(2n+1))}{\pi(2n+1)} \\ &= \Phi_N(\omega) + \Psi_N(\omega). \end{aligned}$$

where  $\Phi_N(\omega) = \frac{4}{N} \sum_{n=0}^{\frac{N}{4}-1} \left\{ \cot\left(\frac{\pi}{N}(2n+1)\right) - \frac{N}{\pi(2n+1)} \right\} \sin(\omega(2n+1))$  and  $\Psi_N(\omega) = \frac{4}{\pi} \sum_{n=0}^{\frac{N}{4}-1} \frac{\sin(\omega(2n+1))}{\pi(2n+1)}$ .

It is well known that for  $N \rightarrow \infty$ ,  $\Psi_N(\omega)$  converges uniformly everywhere except at multiples of  $\pi$ , to a unit valued square wave with period  $2\pi$ . We claim that  $\Phi_N(\omega)$  for  $N \rightarrow \infty$ , converges uniformly everywhere except at multiples of  $\pi$ , to zero. In order to prove this, we consider the interval  $[0, 2\pi]$ . Define  $b_n^N = \frac{N}{\pi(2n+1)} - \cot\left(\frac{\pi}{N}(2n+1)\right)$ , for  $0 \leq n \leq \frac{N}{4} - 1$ . We first need to show that  $b_0^N \leq b_1^N \leq \dots \leq b_{\frac{N}{4}-1}^N \leq \frac{2}{\pi}$ . This is seen as follows: Let  $g(x) = \frac{1}{x} - \cot(x)$ , for  $0 < x < \frac{\pi}{2}$ . Then  $g'(x) = -\frac{1}{x^2} + \frac{1}{\sin^2(x)} > 0$ . Therefore  $g$  is an increasing function. The l'hôpital theorem implies  $g \rightarrow 0$  as  $x \rightarrow 0^+$ . Clearly  $x < \frac{\pi}{2}$  implies  $g(x) < g\left(\frac{\pi}{2}\right) = \frac{2}{\pi}$ . Now we note that  $b_n^N = g\left(\frac{(2n+1)\pi}{N}\right) \in (0, \frac{\pi}{2})$  which completes this proof.

We now complete proof of the claim. First, it can be easily shown that

$$\forall \omega \in [0, 2\pi], \exists M_\omega \geq 0, \forall m \leq \frac{N}{4} - 1, \left| \sum_{n=m}^{\frac{N}{4}-1} \sin((2n+1)\omega) \right| \leq M_\omega,$$

with the estimation:  $M_0 = M_\pi = M_{2\pi} = 0$ . In general,  $M_\omega \leq \frac{C}{\min(|\omega|, |\omega-\pi|, |\omega-2\pi|)}$ , where  $C$  is a positive constant. We now apply the Dirichlet test to  $\sum_{n=0}^{\frac{N}{4}-1} b_n^N \sin((2n+1)\omega)$  but sum it backward (going from  $n = \frac{N}{4} - 1$  to  $n = 0$ ). The Dirichlet test implies that  $\left| \sum_{n=0}^{\frac{N}{4}-1} b_n^N \sin((2n+1)\omega) \right| \leq b_{\frac{N}{4}-1}^N M_\omega \leq \frac{4}{\pi} M_\omega$ . Therefore  $|\Phi_N(\omega)| \leq \frac{16M_\omega}{N\pi} \rightarrow 0$  as  $N \rightarrow \infty$ . This completes proof of the claim.

Hence  $f(\omega)$  converges uniformly to 1 in  $(0, \pi)$  and uniformly to  $-1$  in  $(\pi, 2\pi)$ . Since  $f(\omega)$  is periodic with period  $2\pi$ , it therefore, converges uniformly to 1 in  $(0, \pi)$  and uniformly to  $-1$  in  $(-\pi, 0)$ . This conclude the proof of the first part of Theorem 1. For proof of pointwise convergence to 1, we observe that for  $\omega = 0$  and  $\omega = \pi$ ,  $|Z(e^{j\omega})| = 1$  for all  $N$ . Therefore  $|Z(e^{j\omega})|$  converges pointwise to 1 for  $\omega = 0$  and  $\omega = \pi$  as  $N \rightarrow \infty$ . This conclude the proof of Theorem 1.

## ACKNOWLEDGEMENT

We acknowledge assistance provided by Professor Michael Wilson of the UVM Department of Mathematics and Statistics, in helping derive the proof for convergence in Theorem 1.

## References

- [1] M. Elfataoui, G. Mirchandani, "A Frequency Domain Method for Generation of Discrete-Time Analytic Signals," Accepted October 2005. To appear, *IEEE Trans. Signal Processing*. [www.cems.uvm.edu/~mirchand/publications/ehilbert2.pdf](http://www.cems.uvm.edu/~mirchand/publications/ehilbert2.pdf)
- [2] M. Elfataoui, G. Mirchandani, "Discrete-Time Analytic Signals With Improved Shiftability," *Proceedings, ICASSP 2004*, Montreal, CA. pp. II-477 - II-480, May 2004.
- [3] Mohamed Elfataoui, "Discrete-time Analytic Signals With Improved Shiftability." M.Sc. Thesis, The University of Vermont, Feb. 2004. [www.cems.uvm.edu/~mirchand/publications/me.pdf](http://www.cems.uvm.edu/~mirchand/publications/me.pdf).

- [4] Felix C. A. Fernandes, “*Directional, Shift-Insensitive, Complex Wavelet Transforms with Controllable Redundancy.*” Ph.D. Thesis, Rice University, Jan. 2002.
- [5] S. L. Hahn: *Hilbert Transforms in Signal Processing*, Artech House, Norwood, MA, Dec. 1996.
- [6] N. Kingsbury, “Shift Invariant Properties of the Dual-tree Complex Wavelet Transform, *Proceedings ICASSP 1999*, vol. 3, pp. 1221-1224, March 1999.
- [7] S. Mallat: *A Wavelet Tour of Signal Processing, 2nd edition*, Academic Press, London, UK, Sep. 1999.
- [8] S.L. Marple, Jr., “Computing the Discrete-time Analytic Signal via the FFT,” *IEEE Trans. Signal Processing*, vol.47, No.9, pp. 2600-2603, Sep. 1999.
- [9] S.K.Mitra, *Digital Signal Processing - A Computer-Based Approach*, McGraw-Hill, New York, N.Y. Third Edition, 2006.
- [10] A. Oppenheim, R. Schafer, *Discrete-time Signal Processing*, Prentice Hall, Second Edition, 1999.
- [11] A. Reilly, G. Frazer and B.Boashash, “Analytic Signal Generation - Tips and Traps,” *IEEE Trans. Signal Processing*, vol. 42, No.11, pp. 3241-3245, Nov. 1994.
- [12] I.W.Selesnick, “Hilbert Transform Pairs of Wavelet Bases,” *IEEE Signal Processing Letters*, vol.8, No.6, pp. 170-173, Jun. 2001.
- [13] E. P. Simoncelli, W.T.Freeman, E. H. Adelson, and D. J. Heeger, “Shiftable multi-scale transforms,” *IEEE Trans. Inform. Theory*, 38(2), pp. 587-607, Mar. 1992.
- [14] G. Strang, T. Nguyen: *Wavelets and Filter Banks*, Wellesley-Cambridge Press, Wellesley, MA, 1996.

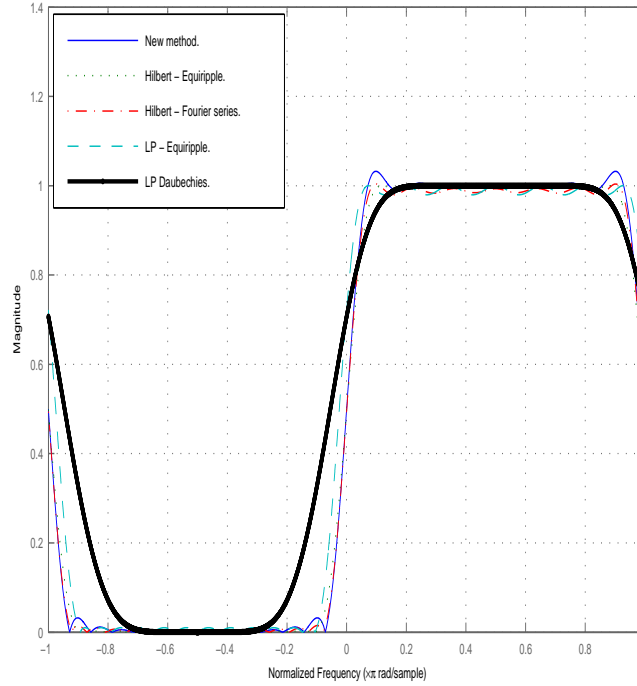


Figure 1: Magnitude frequency response of the five methods.

Ratio of new method and	Level-1 highpass	Level-2 highpass	Level-3 highpass	Level-3 lowpass
LP_daub	0.00017	0.73242	0.34227	0.07561
HT_windowed	0.03168	0.89389	0.87695	0.70610
HT_equiripple	0.09391	0.87422	0.84777	0.65434
LP_equiripple	Inf	0.71158	0.79030	0.07561

Table 1: Ratio of Total Variation with an impulse function.

Ratio of new method and	Level-1 highpass	Level-2 highpass	Level-3 highpass	Level-3 lowpass
LP_daub	0.99311	0.95226	0.56999	0.79540
HT_windowed	0.99796	1.00291	1.02911	1.05536
HT_equiripple	0.97564	0.99394	1.01776	1.09391
LP_equiripple	0.99228	0.99975	1.01105	0.79540

Table 2: Ratio of Total Variation with a step function.

Ratio of new method and	Level-1 highpass	Level-2 highpass	Level-3 highpass	Level-3 lowpass
LP_daub	0.99682	0.98198	0.96633	1.16566
HT_windowed	1.00550	0.98648	0.99835	1.03330
HT_equiripple	0.98464	0.97623	0.98521	1.06701
LP_equiripple	1.00345	0.98749	0.99204	1.16566

Table 3: Ratio of Total Variation with a fractal signal.

Ratio of <i>hilbert</i> and	L-1 highpass	L-2 highpass	L-3 highpass	L-3 lowpass
<i>hilbert</i>	0.78302	1.01261	0.98746	0.77648

Table 4: Ratio of Total Variation with an impulse function.